J. Membrane Biol. 92, 57–74 (1986)

The Journal of
Membrane Biology

Volume, pH, and Ion-Content Regulation in Human Red Cells: Analysis of Transient Behavior with an Integrated Model

Virgilio L. Lew and Robert M. Bookchin
Physiological Laboratory, Cambridge University, United Kingdom, and Albert Einstein College of Medicine, Bronx, New York 10461

Summary. A basic mathematical model of human red cells is presented which integrates the charge and nonideal osmotic behavior of hemoglobin and of other impermeant cell solutes with the ion transport properties of the red cell membrane. The computing strategy was designed to predict the behavior of all measurable variables in time in ways that optimize comparison with experimentally determined behavior. The need and applications of such a model are illustrated in three separate examples covering different areas of experimentation in the physiology and pathophysiology of red cells.

Key Words red cells · volume regulation · pH regulation · ion transport · sickle-cell anemia red cells · Ca^{2+}-sensitive K channels

Introduction

There is much information and substantial agreement about many aspects of red cell transport, pH control and volume regulation. The nonideal osmotic behavior of hemoglobin [1, 19, 20, 27, 39, 59, 61], the change in the net charge on the impermeant cell ion with pH [14, 18, 27, 37], the kinetics and turnover rates of the main monovalent ion transporters [2, 15, 22, 25, 34, 47, 60], and the operation of the Jacobs-Stewart cycle [27, 38, 47, 48] are all now well characterized, though in different, often noncomparable experimental conditions. Some transport properties of red cell membranes have been used in models designed to analyze limited aspects of the steady-state or transient behavior of the cells [8, 35, 64, 65]. There is, however, no framework that integrates the various known features of red cell function into a single model. Without such an integrated model we are unable to predict those aspects of red cell behavior which depend critically on the interaction of diverse functions. Apparently simple questions, concerning the rate and extent of red cell swelling, shrinkage, or pH change under different conditions, cannot be answered precisely. We cannot, for instance, discern whether the expressions describing the charge and nonideal osmotic properties of hemoglobin, formulated with nystatin-treated red cells [14, 18, 27], are also valid in a variety of physiological, pathological, and experimental conditions. Without a model that incorporates those expressions, their influence on cell behavior cannot be predicted, and measured behavior cannot readily be used to correct or refine those expressions.

We introduce here an integrated mathematical model of a human red cell and a method which allows us to compute its transient behavior following perturbations, in a manner analogous to the sequence one normally follows in common experiments with intact cells. This endows the model with the flexibility to reproduce any experimental design, thus optimizing direct quantitative comparison between measured and predicted results. The model, whose basic components are represented in Fig. 1, integrates the nonideal osmotic behavior of hemoglobin [27, 39, 59] with the H^+-binding properties of the impermeant cell ions, as found in nystatin-induced equilibrium experiments [14, 18, 27], and with explicit formulations of the kinetics, when known, or of kinetic alternatives, for the various permeant ion transport pathways.

In the development of this model we have sought to combine economy and reliability in the choice of initial parameters, mathematical simplicity in the selection of equations, and maximal flexibility in the design of the computing strategy. The model is thus a basic, perhaps the simplest possible, integrated representation of the transport, pH and volume regulatory functions of an intact red cell.

We have chosen three examples which pose specific questions designed to illustrate the use of the model. These are analyzed in detail in "Results and Discussion." As presented here, the model has the minimal number of components required to an-

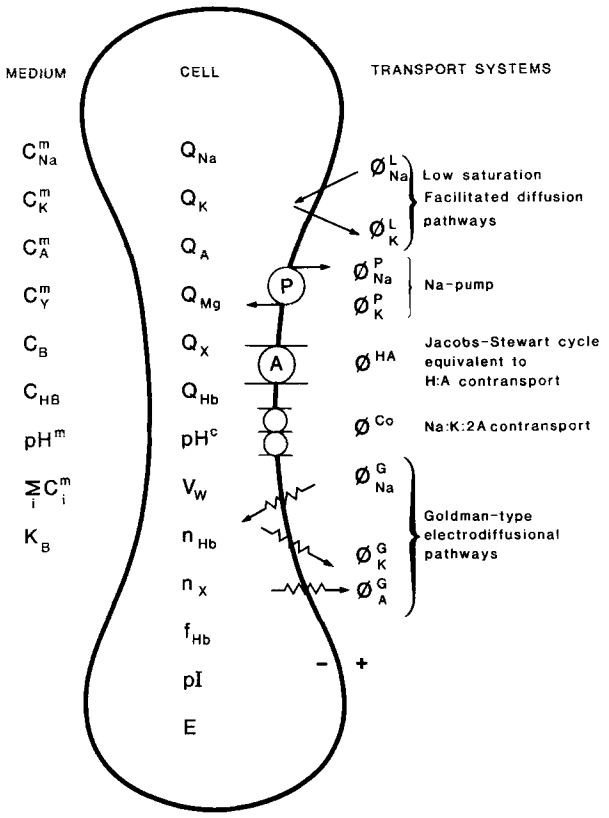

Fig. 1. Variables and flux components of the red cell model

swer these questions. It is, however, open and flexible enough to incorporate any changes and extensions necessary to investigate other specific aspects of intact cell behavior which are or become amenable to experimental test.

Glossary of Symbols and Definitions, List of Model Equations, and Equation-Index for the Computations of the Reference State and of Transients

Q_i:	Amount of solute i in one liter of original packed cells (mmol/loc).
$Q_{(-)}$:	Net charge on impermeant cell ion (mEq/loc).
C_i^c, C_i^m:	Concentration of solute i in cell water (^{c}) or in extracellular medium (m) (molar, M, for H ions; mM for all other solutes).
Subscript i:	Stands for all solutes or for any subset of solutes among: Na, K, Mg, A, Hb, X, Y, B, HB and H.
Na, K, Mg, H:	Sodium, potassium, magnesium and hydrogen ions.
Hb:	Hemoglobin.
A:	Permeant anion.
X:	Impermeant intracellular anion assumed to be nonprotonizable within intracellular pH range explored in present simulations.
Y:	Impermeant extracellular monovalent anion (gluconate, for instance).
B:	Impermeant extracellular H-buffer (Hepes-like, in present simulations).
HB:	Protonized form of extracellular H-buffer.
K_B:	Dissociation constant of extracellular H-buffer (M).
n_X, n_{Hb}:	Mean net charge on X and Hb, respectively (Eq/mole).
pH^c, pH^m:	Cell and medium, pH, respectively.
pI:	Isoelectric pH of hemoglobin.
V_w:	Volume of cell water in one liter of original packed cells (l/loc).
MCHC:	Mean corpuscular hemoglobin concentration (g/100 ml of packed cells).
ϕ_i:	Total flux of permeant solute i (mmol/loch).
ϕ_i^P, ϕ_i^L, ϕ_i^G, ϕ^{Co}, ϕ^{HA}:	Partial flux-component of solute i through the Na-pump (P), a low-saturation facilitated diffusion carrier (L), an electrodiffusional constant-field channel (G), an electroneutral Na : K : 2A cotransport (Co), and an electroneutral H : A cotransport (HA) (representing the operation of the Jacobs-Stewart cycle) (mmol/loch).
P_i^L, P_i^G:	Permeability constant of solute i through facilitated diffusion (L) and electrodiffusional (G) pathways (hr $^{-1}$).
k_{Co}, k_{HA}:	Turnover rate constants for the Na : K : 2A (Co) and for the H : A (HA) cotransports.
z_i, F, R, T, E:	Valence of ion i, Faraday constant, gas constant, absolute temperature, and membrane potential (mV), respectively.
Ht:	Original volume-fraction of cells in cell suspension (hematocrit/100).
Dt:	Integration interval (hr).
a:	Net negative charge on hemoglobin when $pH^c = pI + 1$ (Eq/mole). Slope of the proton titration curve of hemoglobin.
f_{Hb}:	Osmotic coefficient of hemoglobin.
b, c:	Virial coefficients of linear and quadratic terms, respectively, in empirical equation for f_{Hb}.
d:	Compensating factor in kinetic definition of Na : K : 2A cotransport to secure $\phi^{Co} = 0$ in reference state.
ϕ_{max}^{Na}:	Saturated Na efflux through the Na pump (mmol/loch).
f_{Dt}:	Integration interval factor.
f_G:	Fraction of the net passive Na and K fluxes, which is electrodiffusional in the reference state.
DV_w:	Change in the volume of cell water per unit original volume of cells during one integration interval (l/loc).
DQ_i:	Change in the intracellular amount of solute i per unit original volume of cells during one integration interval (mmol/loc).
r_A, r_H:	Ratio between external and internal per-

meant anion concentrations (r_A) or between internal and external hydrogen ion concentrations (r_H).

Superscripts (o), (t) and ($t-Dt$) on a variable indicate the value of that variable in the original reference steady-state (o), at any subsequent time (t), or at the preceding computed time ($t-Dt$). The absence of a time-indicating superscript on any variable is equivalent to the superscript (t).

Fundamental Equations of the Red Cell Model

1. Isotonicity

$$f_{Hb}Q_{Hb} + Q_{Na} + Q_K + Q_{Mg} + Q_X = V_w(C^m_{Na} + C^m_K + C^m_A + C^m_B + C^m_Y)$$

2. Initial electroneutrality

$$Q^o_{Na} + Q^o_K + 2Q_{Mg} - Q^o_A + n^o_{Hb}Q_{Hb} + n_X Q_X = 0$$

3. Nonideal osmotic behavior of hemoglobin

$$f_{Hb} = 1 + b \cdot Q_{Hb}/V_w + c \cdot Q^2_{Hb}/V^2_w$$

4. H^+-buffer behavior of hemoglobin

$$n_{Hb} = a(pH^c - pI)$$

5. Flux equations

$$\phi_{Na} = \phi^P_{Na} + \phi^L_{Na} + \phi^G_{Na} + \phi^{Co}_{Na}$$
$$\phi_K = \phi^P_K + \phi^L_K + \phi^G_K + \phi^{Co}_K$$
$$\phi_A = \phi^G_A + \phi^{HA}_A + \phi^{Co}_A$$
$$\phi_H = \phi^{HA}_H$$

6. Maintenance of electroneutrality

$$\Sigma z_i\phi_i = 0$$

7. Computation of transients

$$DQ_i = \phi_i \cdot Dt$$

8. Redistribution of permeant solutes between cells and suspending medium

$$C^{m(t)}_i = C^{m(t-Dt)}_i(1 + Ht/(1 - Ht))DV_w) - (Ht/(1 - Ht))DQ_i$$

Definitions

$$C^c_i = Q_i/V_w \quad \text{(D1)}$$
$$\phi_i = DQ_i/Dt \quad \text{(D2)}$$
$$C^{c,m}_H = \exp_{10}(-pH^{c,m}) \quad \text{(D3)}$$
$$pH^{c,m} = -\log C^{c,m}_H \quad \text{(D4)}$$
$$r_A = C^m_A/C^c_A \quad \text{(D5)}$$
$$r_H = C^c_H/C^m_H = \exp_{10}(pH^m - pH^c) \quad \text{(D6)}$$
$$Q_{(-)} = n_{Hb} \cdot Q_{Hb} + n_X \cdot Q_X + 2 \cdot Q_{Mg} \quad \text{(D7)}$$
$$DV_w = V^{(t)}_w - V^{(t-Dt)}_w \quad \text{(D8)}$$
$$DQ_i = Q^{(t)}_i - Q^{(t-Dt)} \quad \text{(D9)}$$
$$f_G = \phi^G_{Na}/(\phi^G_{Na} + \phi^L_{Na}) = \phi^G_K/(\phi^G_K + \phi^L_K) \quad \text{(D10)}$$
$$\phi^{Co}_A = 2\phi^{Co}_{Na} = 2\phi^{Co}_K \quad \text{(D11)}$$
$$\phi^{HA}_H = \phi^{HA}_A \quad \text{(D12)}$$
$$\Sigma C^m_i = C^m_{Na} + C^m_K + C^m_A + C^m_B + C^m_Y \quad \text{(D13)}$$
$$MCHC = (MCHC)^o(V^o/V) \quad \text{(D14)}$$

List of Model Equations

Description	Equations Nos.
1. Titratable charges in cells and medium	(1), (14)
2. Net charge on impermeant cell ion	(D7), (19), (34), (35)
3. Osmotic coefficient of hemoglobin	(2)
4. Flux equations	(3) to (12); (D11), (D12)
5. Isotonicity	(17), (24)
6. Electroneutrality	(13), (18), (20)
7. Cell and medium pH	(36), (40), (41)
8. Cell volume	(24), (25), (26)
9. Solute and water shifts between cells and medium	(28), (38), (39)
10. Integration interval	(23)

Computation of the Reference State

Step	Values set or computed	From
1.	Initial cell values and experimental conditions	Table 1
2.	C^{mo}_{HB}, C^{mo}_A	Eqs. (14), (13)
3.	r^o_A, r^o_H, pH^{co}	$\phi^{HAo} = 0$; Eq. (15)
4.	E^o	Eq. (16)
5.	Q_X	Eq. (17)
6.	f^o_{Hb}	Eq. (2)
7.	n^o_{Hb}	Eq. (1)
8.	n_X	Eq. (18)
9.	$Q^o_{(-)}$	Eq. (19)
10.	ϕ^{max}_{Na}	ϕ^{Po}_{Na}, Table 1; Eq. (7)
11.	P^L_{Na}, P^L_K	set f_G; $\phi^o_{Na} = 0$; $\phi^o_K = 0$
	P^G_{Na}, P^G_K	Eqs. (3), (4), (9), (10)
12.	d	$\phi^{Coo} = 0$; Eq. (11)
13.	P^G_A, k_{Co}, k_{HA}	values set within desired range

Computation of Transients

Step	Values set or computed	From
1.	Set perturbation in parameter or concentrations	
2.	E	Eq. (20)
3.	ϕ_i^G	Eq. (10)
4.	ϕ^{Co}, ϕ^{HA}	Eqs. (11), (12)
5.	ϕ_i	Eqs. (3), (4), (5)
6.	Q_i	Eqs. (21), (22)
7.	V_w	Eq. (24)
8.	C_i^c, C_i^m	Eqs. (27), (28)
9.	$Q_{(-)}$, pH^c	Eqs. (34), (35), (36)
10.	C_{HB}^m, C_B^m, pH^m	Eqs. (38) to (41)
11.	Test for printing intermediate results, for changes in conditions or for end of experiment.	
12.	Go to step 2.	

Structure of the Red Cell Model

Following the strategy introduced for the analysis of transporting epithelial cells [55], the computations of the RCM were organized in two main stages. The first stage uses a minimal set of well-characterized human red cell values and standard experimental conditions to define an initial reference steady state which represents, to a good approximation, the physiological condition of fresh intact red cells at the start of experiments. The second stage computes the evolution in time of all the variables in the system following a specified perturbation.

In this section we discuss the principles followed in the design of the computing strategy and present all technical details required to reproduce the computations.

Explanation of Symbols and Equations

Cell contents of water (V_w) and of solutes (Q_i) are expressed in liters or millimoles (mmol) per liter original cells (liter/loc or mmol/loc), respectively. One liter of original cells is meant to represent a normalized quantity corresponding to 1 liter of fully packed fresh, normal human red cells containing 340 g hemoglobin. This corresponds to a mean corpuscular hemoglobin concentration (MCHC) of 34 g/dl. By definition, the concentration of solute i in cell water (C_i^c) is given by $C_i^c = Q_i/V_w$ and is expressed in mmol/liter (mM), as is the concentration of solutes in the extracellular medium (C_i^m). The solutes considered in this model, and represented in the equations by the subscript i or by that of the specific symbols, are of two categories: permeant and impermeant. The permeant solutes are Na, K, the diffusible anion A (Cl^-, HCO_3^-, SCN^-, or any combination of highly permeant monovalent anions) and hydrogen ions, H^+. The impermeant solutes are: Mg^{2+}, hemoglobin (Hb), cell solutes other than hemoglobin (X), one unspecified extracellular solute (Y), convenient for simulating isotonic replacement experiments, and an extracellular proton-buffer (B), Hepes-like in the examples reported in this paper, with proton-dissociation constant K_B and protonized form HB. The mean net charge on Hb and X is represented by n_{Hb} and n_X, respectively, and is expressed in units of equivalents per mole (eqiv/mole). We followed Dalmark [18] in the interpretation of Eq. (1) and in attributing the protonizable groups in the red cell to those on the hemoglobin molecule, n_{Hb}. The charges represented by n_X are assumed to remain deprotonized, and therefore constant, within the range of cell pH (pH^c) covered by the present simulations. Medium pH is indicated by pH^m, and hydrogen ion concentrations in cell and medium are, by definition, $C_H^{c,m} = \exp_{10}(-pH^{c,m})$. $Q_{(-)}$ is defined by $Q_{(-)} = n_{Hb} \cdot Q_{Hb} + n_X \cdot Q_X + 2Q_{Mg}$ and represents the total net charge on the impermeant cell ion, in units of milliequivalents per liter original cells (meq/loc). The protonizable charge, n_{Hb}, represents the intracellular H^+ buffer. The titration curve of nystatin-treated red cells [18, 27] shows that, in the pH^c range between about 6 and 8, the behavior of the protonizable groups may be adequately described by the equation:

$$n_{Hb} = a(pH^c - pI) \tag{1}$$

where a is a coefficient representing the slope of the titration curve (in meq/mmol), and pI is the intracellular pH at which $n_{Hb} = 0$.

According to Dalmark [18] and to Freedman and Hoffman [27] the value of a is about -10 equiv/mole. When $pH^c > pI$, the net charge on hemoglobin is negative and when $pH^c < pI$, it becomes positive, as expected from the relative numbers and pKs of uncharged and negatively charged H^+-reactive groups on the hemoglobin molecule. Use of Eq. (1) implies that n_{Hb} is not directly dependent on cell volume. There has been controversy on this point [27, 31, 32, 38]. The evidence supports volume-independence to any extent that might influence cell volume regulation. Minor effects, however, cannot be ruled out. In concentrated hemoglobin solutions small pH changes with changes in hemoglobin concentration have been reported [5] and interpreted in terms of changes in the pK of protonizable histidine residues at critically close intermolecular distances [5].

Following McConaghey and Maizels [59] and Freedman and Hoffman [27], we define the change in the osmotic coefficient of hemoglobin with cell volume using the empirical equation:

$$f_{Hb} = 1 + b \cdot Q_{Hb}/V_w + c \cdot Q_{Hb}^2/V_w^2 \tag{2}$$

with virial coefficients b and c. The effects of changes in the definition of f_{Hb} are analyzed in the simulated experiments of Fig. 6.

The superscript (^{o}) on a variable represents its value in the initial reference steady state. The superscript (^{t}), or simply the absence of temporal superscripts, (^{o}) or (^{t}), represents the value of that variable at any other time. Dt represents the incremental interval used for the computation of the transients. DV_w is defined by $DV_w = V^t - V^{(t-Dt)}$ and represents the change in cell volume during each incremental interval. The relative volume of suspension occupied by the cells in the initial reference state is indicated by Ht, which represents the initial hematocrit.

The Flux Equations

For the computation of transients it becomes necessary to provide kinetic definitions for the fluxes of all permeant solutes. Fluxes were expressed in units of mmole per liter original cells per hour (mmol/loch) to allow direct comparison with common experimental practice. In addition, expression of fluxes per unit volume of original cells is particularly useful because it allows treatment of permeability and rate constants as real constants, independent of the area/volume ratio of the cells in the reference state. The fluxes per unit real volume of cells at each instant of

time can easily be calculated by dividing the fluxes expressed per unit original cell volume by the relative volume of the cells at that time (the area of transporting membrane is assumed to remain constant). The same correction would apply in the calculation of the instantaneous value of the permeabilities and rate constants used in the flux equations.

Net fluxes into the cells were defined as positive. The total net flux of solute i is indicated by ϕ_i. Partial flux components are identified by superscripts P, L, G, Co and HA, representing fluxes through the Na pump (P), a low-saturation facilitated diffusion carrier (L), a constant-field electrodiffusional path (G), a neutral Na : K : 2A cotransport (Co), and a neutral H : A cotransport (HA), meant to represent the operation of the Jacob-Stewart cycle [48].

The equations describing the total fluxes are:

$$\phi_{Na} = \phi^{P}_{Na} + \phi^{L}_{Na} + \phi^{G}_{Na} + \phi^{Co}_{Na} \quad (3)$$

$$\phi_{K} = \phi^{P}_{K} + \phi^{L}_{K} + \phi^{G}_{K} + \phi^{Co}_{K} \quad (4)$$

$$\phi_{A} = \phi^{G}_{A} + \phi^{HA}_{A} + \phi^{Co}_{A} \quad (5)$$

$$\phi_{H} = \phi^{HA}_{H}. \quad (6)$$

The following equations define the kinetics of the various flux components used here:

$$\phi^{P}_{Na} = -\phi^{max}_{Na}(C^{c}_{Na}/(C^{c}_{Na} + 0.2(1 + C^{c}_{K}/8.3)))^{3} (C^{m}_{K}/(C^{m}_{K} + 0.1(1 + C^{m}_{Na}/18)))^{2} \quad (7)$$

$$\phi^{P}_{K} = -\phi^{P}_{Na}/1.5. \quad (8)$$

Equation (7) describes the Na pump-mediated Na efflux and incorporates the known competitive inhibitory effects of internal K and external Na [12, 31]. ϕ^{max}_{Na} represents the Na efflux through a Na pump saturated with internal Na and external K, at the ATP levels of normal red cells. Equation (8) incorporates the known 3 : 2 stoichiometry of the pump for Na : K exchange.

The passive flux components were defined by:

$$\phi^{L}_{i} = -P^{L}_{i}(C^{c}_{i} - C^{m}_{i}) \quad (9)$$

$$\phi^{G}_{i} = -P^{G}_{i} \cdot (z_i FE/RT)((C^{c}_{i} - C^{m}_{i} \cdot \exp(-z_i FE/RT))/(1 - \exp(-z_i FE/RT)) \quad (10)$$

$$\phi^{Co} = -k_{Co}((C^{c}_{A})^{2} \cdot C^{c}_{Na} \cdot C^{c}_{K} - d \cdot (C^{m}_{A})^{2} \cdot C^{m}_{Na} \cdot C^{m}_{K}) \quad (11)$$

$$\phi^{HA} = -k_{HA}(C^{c}_{A} \cdot C^{c}_{H} - C^{m}_{A} \cdot C^{m}_{H}). \quad (12)$$

Unlike the Na pump-mediated fluxes, the true kinetics of the flux components defined by Eqs. (9) and (10) are not known. Moreover, Eq. (9) probably lumps together a variety of different transporters. Equations (9) and (10), therefore, may represent the simplest mathematical options, but they are also unrealistic and arbitrary. We must therefore consider how this may affect the predictions of the model.

In short-term experiments in which the K or Na permeabilities are increased orders of magnitude above normal, through activation of Ca-sensitive K channels [60] or by addition of ionophores, as well as in experiments where cell volume and composition changes are caused by fast net fluxes through the Jacobs-Stewart mechanism, the short-term behavior predicted by the model will be little affected by the kinetics of the slow Na/K transporters. The results of such "rapid" experiments are analyzed in detail below. In slow, long-term experiments, on the other hand, the true kinetics of the Na and K transporters becomes important.

In recent years, much information has been gained on the existence and pharmacological reactivity of a variety of transporters which link, in different ways, the fluxes of all monovalent ions in red cells: H, Na, K and Cl(A) [6, 7, 13, 22, 23, 36, 37, 53, 68, 69]. Little is known yet about the precise kinetics of these transporters. Some are modulated by cell volume or pH and may thus, in turn, alter the value of these variables [6, 7, 13, 53]. The present model provides easy ways of exploring the effects of such transporters simply by redefining Eqs. (3) to (6) and (9) to (12), as exemplified here with the incorporation of a Na : K : 2A cotransporter (*see below*) [13, 22, 23, 36, 37]. Since all transport systems operate in parallel in the membrane, their inclusion in the model is simply done by adding terms to the flux equations of the transported ions. Such additions, which may include complex kinetics and volume/pH feedback reactions, will not change the basic structure of the model or the sequence of the computations. As shown below, in each integration cycle the individual ion fluxes are computed sequentially using whichever expressions define Eqs. (3) to (6). Therefore, these equations can be modified without altering any other part of the program.

Ideally, a comprehensive red cell model should contain the kinetics of all the identified transporters. In practice, however, since we ignore the precise kinetics of any transporter other than the Na pump, a comprehensive model would have to be extremely arbitrary and necessarily unrealistic. This need not hamper gradual progress towards more realistic and complete models as long as we do not attempt to start with a comprehensive model, and just follow a few simple and practical rules. Sensible use of the model as a tool to test hypotheses and guide research requires that we begin with only those terms in the flux equations which represent either well-characterized kinetics (such as that of the Na pump) or uncharacterized but essential flux components. The number of these components as well as that of the parameters used in the initial kinetic descriptions should be kept to a minimum. Comparison between predicted and measured behavior can then be used to correct, refine and extend the initial descriptions to improve the fit. In the first example below we attempt to answer a specific theoretical point by exploring the effects of different kinetic definitions of the passive components of the Na and K fluxes.

In order to generate different kinetics we fixed the parameter f_G, defined as the proportion of $\phi^{G}_{Na,K}$ to $(\phi^{G}_{Na,K} + \phi^{L}_{Na,K})$ flux components, at a value of either 0.1 or 0.9; this has the effect of assigning the fraction of the passive Na and K fluxes through potential-sensitive diffusional pathways, as either 10%, the value that probably best represents the physiological condition [2, 54], or as 90%. The size of the fluxes predicted by these two kinetic alternatives approximately spans the range of Na and K fluxes which have been measured in experiments relevant to the examples analyzed. The effects of these specific kinetics will be analyzed below in the presence of a cotransport system such as that described by Eq. (11).

In Eqs. (9) and (10), $P^{L,G}_{i}$ define permeability coefficients in units of h^{-1}; z_i is the valence of ion i; E, the membrane potential (in mV); and F/RT lumps the Faraday constant (F), ideal gas constant (R) and absolute temperature (T) into a single constant whose value at 37°C was fixed at 0.037 mV^{-1}. k_{Co} and k_{HA} define the turnover rate of the respective cotransports. The dimensionless factor d in Eq. (11) secures that $\phi^{Co} = 0$ in the reference steady state, so that the diffusible anion is at electrochemical equilibrium. The computed value of d turns out to be very near 1 (*see* Table 2), indicating that if such cotransport exists in human red cells, it must be at or very close to equilibrium under physiological conditions. Equation (11) is the simplest mathematical

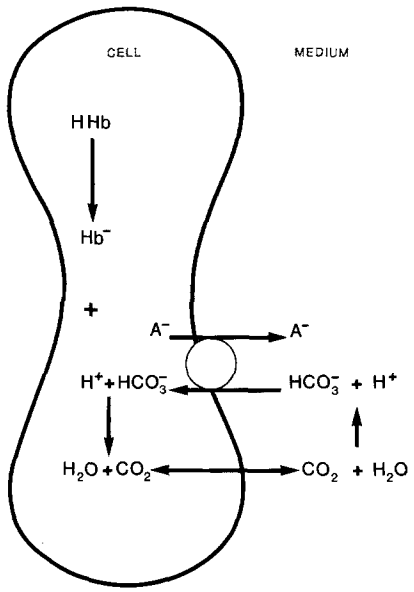

Fig. 2. Operation of the Jacobs-Stewart cycle after isotonic replacement of the permeant anion by an impermeant anion in the suspending medium

Table 1. Values of parameters and variables used for the computation of the reference state

Cell values	
a	−10 mEq/mmol
b	0.0645
c	0.0258
pI	6.85
Q_{Hb}	5 mmol/loc
Q_{Mg}	2.5 mmol/loc
C^{co}_{Na}	10 mmol/lcw
C^{co}_{K}	140 mmol/lcw
C^{co}_{A}	95 mmol/lcw
V^{o}_{w}	0.7 liter/loc
ϕ^{P}_{Na}	2.6 mmol/loc · hr
Experimental conditions	
Ht	0.1 (equivalent to a hematocrit of 10%)
C^{mo}_{Na}	140 mM
C^{mo}_{K}	5 mM
pH^{mo}	7.40
C^{mo}_{B}	10 mM
K_B	$10^{-7.55}$ M
C^{mo}_{y}	10 mM

expression for a neutral Na:K:2A cotransport such as that found in red cells from a variety of species and best characterized in avian and ferret red cells [23, 36, 37, 50].

Equation (12) describes the operation of the Jacobs-Stewart mechanism [48], as illutrated in the example of Fig. 2. In normal conditions the anion carrier of red cells maintains an equilibrium defined by $r_A = C^m_A/C^c_A = r_H = C^c_H/C^m_H$, which applies to any permeable anion and also to the sum of all permeable anions present in the system [30]. For the experiments analyzed here, A may represent a single highly permeant anion like Cl^-, for instance, or any combination of Cl^- and HCO_3^- anions. If an outward concentration gradient of A is set up, thus perturbing the initial equilibrium, even contaminant traces of HCO_3^- ions will provide a rapid exchange of HCO_3^- for Cl^- through the powerful anion exchanger (Fig. 2). The CO_2 shunt effectively prevents the buildup of intracellular HCO_3^- or the maintenance of meaningful CO_2 gradients. The net result is therefore a 1:1 exit of H and A from the cells with deprotonation of hemoglobin and cell dehydration [4]. This proceeds until a new equilibrium is reached, again defined by $r_A = r_H$. Equation (12) describes this process in terms of a hypothetical A:H cotransport, lumping all the kinetics into a single parameter. k_{HA} represents the turnover of the limiting step in the cycle. Even with only contaminant traces of CO_2 in the cell suspension, the limiting step is likely to be anion carrier turnover. Equation (12) can therefore be extended to test specific carrier kinetics in experiments designed for that purpose.

Computation of the Reference State

Table 1 gives the values of parameters and variables used here to define the reference state. This set of values describes conditions expected in metabolically normal fresh red cells washed and suspended at 10% hematocrit in a medium buffered to pH 7.4 and containing 10 mM of Na gluconate, plasma-like Na and K concentrations, and Cl^-, or Cl^- and HCO_3^-, as the only diffusible anions. The choice of parameters and variables in Table 1 is flexible. The values were chosen to represent a minimal set of reliably measured quantities from which all others could be conveniently derived. Cell pH or anion ratio, for instance, may be preferred to the concentration of A in the cells; but the total number of initial parameters and variables, as given in Table 1, cannot be reduced without removing components of the integrated model.

The values in Table 2 were derived from those in Table 1 as follows:

Electroneutrality in the suspending medium requires that

$$C^{mo}_A + (C^{mo}_B - C^{mo}_{HB}) + C^{mo}_y = C^{mo}_K + C^{mo}_{Na} \tag{13}$$

where

$$C^{mo}_{HB} = C^{mo}_B(C^{mo}_H/(K_B + C^{mo}_H)). \tag{14}$$

Depending on how the buffered suspending medium is prepared, we may need to solve Eq. (13) for C^{mo}_{Na}, C^{mo}_K or, as with the choice made in Table 1, for C^{mo}_A.

Since $\phi^{AH} = 0$, we can now compute C^{co}_H, pH^{co}, E^o, r^o_A and r^o_H from

$$r^o_A = r^o_H = C^{mo}_A/C^{co}_A = C^{co}_H/C^{mo}_H \tag{15}$$

and from

$$E^o = -(RT/F)\ln r^o_A. \tag{16}$$

Using $Q^o_i = V^o_w \cdot C^{co}_i$, the isotonicity condition

$$Q^o_{Na} + Q^o_K + Q^o_A + Q_{Mg} + f^o_{Hb} \cdot Q_{Hb} + Q_X = V^o_w(C^{mo}_{Na} + C^{mo}_K + C^{mo}_A + C^{mo}_B + C^{mo}_y) \tag{17}$$

allows us to compute Q_X, the only unknown left in Eq. (17). f^o_{Hb} is calculated from Eq. (2) using $V_w = V^o_w$.

Initial electroneutrality in the cells, given by

$$Q^o_{Na} + Q^o_K + 2Q_{Mg} - Q^o_A + n^o_{Hb}Q_{Hb} + n_X Q_X = 0 \quad (18)$$

renders n_X; n^o_{Hb} is calculated from Eq. (1) using pH^{co}. The total initial net charge on the impermeant ion, $Q^o_{(-)}$, can now be calculated from

$$Q^o_{(-)} = n^o_{Hb} \cdot Q_{Hb} + n_X Q_X + 2Q_{Mg}. \quad (19)$$

In the running of the program, $(Q_X + Q_{Mg})$ and $(n_X Q_X + 2Q_{Mg})$ were treated as lumped constants whose value was determined from the isotonicity (Eq. (17)) and electroneutrality (Eq. (18)) conditions. From the choice of initial values in Table 1, $(Q_X + Q_{Mg}) = 21.7$ mmol/loc and $(n_X Q_X + 2Q_{Mg}) = -18.0$ mEq/loc.

With a Q_{Mg} of about 2.5 mmol/loc [24] the content and charge of the remaining nonpermeant cell ion are about 19 mmol/loc and -1.2 mEq/mmol, respectively, values consistent with those reported for the organic and inorganic phosphate pools of metabolically normal red cells [67]. At the resulting pH^c of 7.26, the net charge on hemoglobin is about -4 mEq/mmol. Thus, hemoglobin provides about 20 mEq/loc of negative charge in the reference state. Note that the introduction of Q_X and n_X represents the simplest way to comply with isotonicity and electroneutrality using the values in Table 1.

Using the initial concentrations and membrane potential, it is now possible to solve Eqs. (3) and (4) under reference state conditions, when all net fluxes are zero, to give the values of ϕ^{max}_{Na}, P^L_{Na}, P^L_K, P^G_{Na} and P^G_K. We compute ϕ^{max}_{Na} from Eq. (7). We choose the desired proportion of L to $(L + G)$ flux components for Na and K, f_G, and we then compute P^L_{Na}, P^L_K, P^G_{Na} and P^G_K using Eqs. (9) and (10), with $\phi^o_{Na} = \phi^o_K = 0$. The constant field permeability of the diffusible anion, P^G_A, was varied over the range given in Table 2, to cover the range of experimentally observed values [9, 42, 43].

When computing transients, k_{Co} and k_{HA} were set either at 'off' values of 10^{-9} and 1, or at 'on' values of 10^{-6} and 10^9, respectively, in the units required for dimensional coherence in Eqs. (11) and (12). The 'on' value of 10^9 for k_{HA} was chosen so that ϕ_{HA} would mediate a net anion flux equivalent to 10^4 times the total monovalent cation flux at maximal driving gradient. This is approximately equivalent to the observed anion self-exchange rate through the anion carrier at 25–37°C [9]. The 'on' value of k_{Co} is arbitrary and was set for adequate illustration of the points analyzed below.

Table 2. Values of model parameters and of reference-state variables derived from those in Table 1

$E^o = -8.6$ mV	$C^{mo}_A = 130.9$ mM
$r^o_A = r^o_H = 1.38$	$Q^o_{(-)} = -38.5$ mmol/loc
$pH^{co} = 7.26$	$Q_X = 19.2$ mmol/loc
$f^o_{Hb} = 2.78$	$\phi^{max}_{Na} = 8.99$ mmol/loc hr
$d = 1.05$	$P^G_A = 0.2$ to 200 hr^{-1}
$C^{mo}_{HB} = 5.86$ mM	$n^o_{Hb} = -4.11$ equivalents/mole
	$n_X = -1.19$ equivalents/mole

	$f_G = 0.1$	$f_G = 0.9$
$P^L_{Na}(hr^{-1})$	0.0180	0.0020
$P^L_K(hr^{-1})$	0.0116	0.0013
$P^G_{Na}(hr^{-1})$	0.0017	0.0151
$P^G_K(hr^{-1})$	0.0015	0.0138
	'off'	'on'
k_{Co}	10^{-9}	10^{-6}
k_{HA}	1	10^9

Computation of Transients

A perturbation is represented by a change in one or more of the variables or parameters listed in Tables 1 and 2. For example, full activation of the Ca-sensitive K channels or addition of valinomycin would be represented by an increase in P^G_K. Complete Na-pump inhibition by ouabain would be obtained by making $\phi^{max}_{Na} = 0$. Inhibition of the anion carrier would need reductions in k_{HA} and perhaps also in P^G_A [9, 25]. Changes in the composition or tonicity of the medium are obtained by changing the corresponding C^m_i.

Changes in cell composition should generally be computed by starting at the reference state and simulating the experiment causing those changes. Sometimes, however, we wish to perform simulations on red cells which have already undergone experimental treatments, or on red cells in pathological states, which involve changes in their internal composition. It may be cumbersome or, because of deficient knowledge, difficult to model the process that we need to follow from the normal reference state in order to arrive at the modified condition. We may then wish to bypass the problem by redefining a reference state with abnormal cell volume or contents, which we believe is an accurate representation of the state of the cell before the experiment we want to simulate and analyze. The abnormal reference state becomes an initial assumption, and the simulation simply illustrates the behavior predicted on the basis of that assumption. This procedure may be justified in some instances, but it is important to remember that we may overlook unsuspected changes which would have only become apparent had we been able to compute all transients from the normal reference state.

In order to follow the transient behavior of the model after a perturbation we perform the sequence of computations outlined below.

First, we compute the new value of E from

$$\Sigma z_i \phi_i = 0. \quad (20)$$

This equation states that the algebraic sum of the individual ionic currents through all transporters must be zero [29, 44, 45, 55]. This secures the maintenance of electroneutrality. Equation (20) is implicit in E, and it was solved using the secant iteration algorithm (Hewlett-Packard, HP41 preprogrammed function). Any perturbation represented by a change in the concentrations or parameters contained within the flux Eqs. (7), (9) and (10) will render a value of E different from E^o. The two cotransport equations, having been defined electroneutral, are ignored in the computation of E.

With E, we can now compute each of the ϕ^G flux components and, from Eqs. (3), (4) and (5), all the individual ion fluxes, ϕ_i. With these, we calculate the new values of Q_i using

$$DQ_i = \phi_i \cdot Dt \tag{21}$$

and

$$Q_i^t = Q_i^{(t-Dt)} + DQ_i. \tag{22}$$

These two sets of equations provide the new amount of intracellular solute i per liter original cells at the end of the incremental interval Dt. The use of Eq. (21) assumes that Dt is sufficiently small to secure that ϕ_i does not change significantly within that interval.

In theory, the size of the incremental interval Dt should be infinitely small. In practice, economy of computing time requires that we search, in every cycle, for the highest possible value of Dt which would alter results by less than a specified tolerance limit. These values will depend closely on the rates of all time-dependent processes. There is no universal rule to set the value of Dt for all conditions. The simple relation

$$Dt = f_{Dt}/\Sigma\,|\phi_i| \tag{23}$$

where $\Sigma\,|\phi_i|$ is the sum of the absolute value of all net ionic fluxes and f_{Dt} is an empirical constant, was used in the present computations. Equation (23) links Dt inversely to a maximal estimate of the overall ionic traffic across the cell membrane, as provided by $\Sigma\,|\phi_i|$. f_{Dt} values in the range 0.1 to 0.4 were adequate to keep the results within 1% of those obtained with one hundred-fold smaller f_{Dt} values, at the end of the simulated experiments. This allowed many of the computations to be performed on a portable HP 41C-type calculator. An additional advantage of using Dt as defined by Eq. (23) is that we can automatically obtain printouts of computed values at frequencies proportionate to the rate of change in net ionic fluxes, by instructing the program to print the partial results after a constant number of computing cycles.

By applying the isotonicity condition of Eq. (17) using the new $Q_i = Q_i^t$ values obtained from Eq. (22), we can now compute the new volume of cell water per liter original cells, V_w. We combine Eq. (2) with Eq. (24)

$$f_{\mathrm{Hb}}Q_{\mathrm{Hb}} + \Sigma\, Q_i = V_w \Sigma\, C_i^m \tag{24}$$

where

$$\Sigma\, Q_i = Q_{\mathrm{Na}} + Q_{\mathrm{K}} + Q_{\mathrm{A}} + Q_{\mathrm{Mg}} + Q_X \tag{25}$$

and where $\Sigma\, C_i^m$, the 'isotonic' external concentration, is given by

$$\Sigma\, C_i^m = C_{\mathrm{Na}}^m + C_{\mathrm{K}}^m + C_{\mathrm{A}}^m + C_B^m + C_y^m \tag{26}$$

and solve for V_w, selected as the only real root within the feasible solution range. With V_w we can now compute the new intracellular concentrations from

$$C_i^c = Q_i/V_w. \tag{27}$$

The new concentrations of extracellular ions at the end of each incremental interval, which result from the ionic and water shifts between cells and medium, are computed from

$$C_i^{m(t)} = C_i^{m(t-Dt)}(1 + (Ht/(1 - Ht))DV_w) - (Ht/(1 - Ht))DQ_i \tag{28}$$

Equation (28) was derived as follows: by definition, $C_i^m = M_i/V_s$, where M_i represents the amount of solute i (in mmol) in a given volume V_s of extracellular medium. Therefore,

$$dC_i^m = (1/V_s)dM_i - (M_i/V_s^2)dV_s. \tag{29}$$

By expressing DQ_i and DV_w per liter original cells, the following transformations become valid:

$$V_s = 1 - Ht \tag{30}$$

$$dM_i = -DQ_i \cdot Ht \tag{31}$$

$$dV_s = -DV_w \cdot Ht. \tag{32}$$

Making

$$C_i^{m(t)} - C_i^{m(t-Dt)} = dC_i^m. \tag{33}$$

We can now derive Eq. (28) from Eq. (29) using the substitutions in (30)–(33). The first term in Eq. (28) describes the change in C_i^m due to water shifts from cells to medium. The second term describes the change in C_i^m due to ion shifts and applies only to permeant solutes, where $DQ_i \neq 0$.

Computation of the H^+ concentration in cells and medium requires alternative equations because of the presence of an extracellular buffer and intracellular protonizable groups which bind almost all the transported H^+. The intracellular proton distribution was calculated from

$$DQ_{\mathrm{H}} = \phi^{\mathrm{HA}} \cdot Dt \tag{34}$$

$$Q_{(-)}^{(t)} = Q_{(-)}^{(t-Dt)} + DQ_{\mathrm{H}} \tag{35}$$

$$\mathrm{pH}^c = pI + ((Q_{(-)}^{(t)} - (n_X Q_X + 2Q_{\mathrm{Mg}}))/aQ_{\mathrm{Hb}}) \tag{36}$$

$$C_{\mathrm{H}}^c = \exp_{10}(-\mathrm{pH}^c). \tag{37}$$

The extracellular proton distribution was computed from

$$C_{HB}^{m(t)} = C_{HB}^{m(t-Dt)}(1 + (Ht/(1 - Ht))DV_w) - (Ht/(1 - Ht))DQ_{\mathrm{H}} \tag{38}$$

$$C_B^{m(t)} = C_B^{m(t-Dt)}(1 + (Ht/(1 - Ht))DV_w) \tag{39}$$

$$C_{\mathrm{H}}^m = K_B(C_{HB}^m/(C_B^m - C_{HB}^m)) \tag{40}$$

$$\mathrm{pH}^m = -\log C_{\mathrm{H}}^m. \tag{41}$$

Equation (36) was obtained by combining Eq. (1) with the noninitial form of Eq. (19) and solving for pH^c. Equation (38) is a particular form of Eq. (28), which computes the change in protonized extracellular buffer concentration due to water and proton shifts between cells and medium. Only water shifts affect the total external concentration of the impermeant buffer, as expressed by Eq. (39). Equation (40) is the noninitial form of Eq. (14), which describes the external buffer equilibrium and allows us to compute the new C_H^m and pH^m values (Eq. (41)).

Equation (41) completes the computation of one Dt cycle. With the new C_i^c and C_i^m values, the program now returns to Eq. (20) and repeats the cycle as many times as instructed for the desired length of the simulated experiment. When running the program, breaks are preset for printing or plotting intermediate results and for changing or restoring experimental conditions.

Results and Discussion

In this section we report and analyze the results of simulated experiments chosen to illustrate the application of the integrated model to a diverse sample of conditions. For each example, we first describe the nature of the problem and the questions presented for analysis using the model. The predicted results are then described, and the model is tested by comparison with published experimental results. Finally, we analyze the models' answers to the original questions and discuss the wider implications arising from these predictions.

The display of the results in Figs. 3, 4, 5 and 6 includes the values of the selected variables in the reference state, as given in Tables 1 and 2. Zero-time corresponds either to the start of a final incubation after a reversible perturbation, as in Fig. 3, or to the initiation of a sustained perturbation, as in Figs. 4 to 6. Unless specified otherwise in the figure legend, the red cells were considered to be suspended at 10% hematocrit in the saline buffer described in Table 1.

Factors Controlling the Rate and Extent of Red Cell Volume Changes after Balanced Na/K Gradient Dissipation

Formulation of the Problem

Sickle cell anemia red cells (*SS*) become progressively dehydrated and rigid in the circulation. It is generally believed that the densest cell fraction, mostly irreversibly deformed cells, plays an important role in the generation of hemolytic anemia and microcirculatory occlusion, the two main clinical features in this disease [3]. The densest *SS* cells have lost much more K than they have gained Na [3]. In physiological-like conditions, however, sickling in vitro causes only a balanced K loss and Na gain without measurable cell dehydration [66]. Glader and Nathan [33] and Clark et al. [16] proposed a mechanism by which an initially balanced Na/K change could lead to cell dehydration. They suggested that restoration of the Na/K gradients by a Na pump with a Na : K stoichiometry of about 1.5, in a cell where the diffusible anion provides the charge-balancing flux, ought to cause progressive cell dehydration. Clark et al. [16] tested this hypothesis on nystatin-pretreated normal red cells, and found, whether the cells were initially swelled or shrunk during pretreatment, that as long as cell Na was increased by more than 40 mM, with fairly balanced K loss, they became more dehydrated during a subsequent 20–24 hr incubation as a result of Na pump activity. If all permeability changes had been transient and fully reversible, as Clark et al. [16] imply for the nystatin pretreated cells, the cells should eventually return to their original normal volume and concentrations, since the steady-state solutions show that cell concentrations and volume are uniquely determined for each set of parameters [65]. The theoretical questions, therefore, are: in a cell which has experienced a reversible and transient permeability change leading to balanced Na/K dissipation, what are the expected rates of dehydration and volume restoration? Which factors control each of these processes? Do these processes overlap in time and canel each other, at least partially? Could this be a possible mechanism for sickle cell dehydration?

Results and Analysis

The protocol in the experiment of Fig. 3 simulated that followed by Clark et al. [16] after nystatin treatment of the cells. In their experiments, nystatin treatment of normal red cells was used to induce a substantial increase in cell Na and decrease in cell K concentration with either an initial increase or decrease in cell volume. After removing the ionophore, the cells were incubated in plasma-like media at 37°C and the cell Na, K and water contents were assessed in samples obtained after about 20–24 hr. In the present simulation, we have assumed no initial volume change after a balanced cell Na gain and K loss. Zero-time in Fig. 3 corresponds to the start of this final incubation. C^c_{Na}/C^c_K was changed from 10/140 in the Reference State to the 70/80 value found to consistently result in cell dehydration accompanied by net cation loss during C^c_{Na}/C^c_K recovery [16]. In Fig. 3 we report the results predicted by models with different kinetic definitions for the passive Na and K flux components. We tested kinetic options whereby the electrodiffusional fluxes represented either 10 or 90% of the total passive flux, for model red cells defined with either normal or hyperpolarized membrane potentials. The hyperpolarized cell condition was obtained by setting the cell permeant anion concentration at 30 mM in the reference state. The resulting initial membrane potential and cell pH were −40 mV and 6.8, respectively. The net negative charge on the impermeant cell anion was −84 mEq/loc. We also report the changes predicted in the presence of a Na : K : 2Cl cotransport. As we shall see, these variants represent the main options worth considering in this type of general analysis.

It can be seen (Fig. 3) that for the model variants without active cotransport, the predicted time-

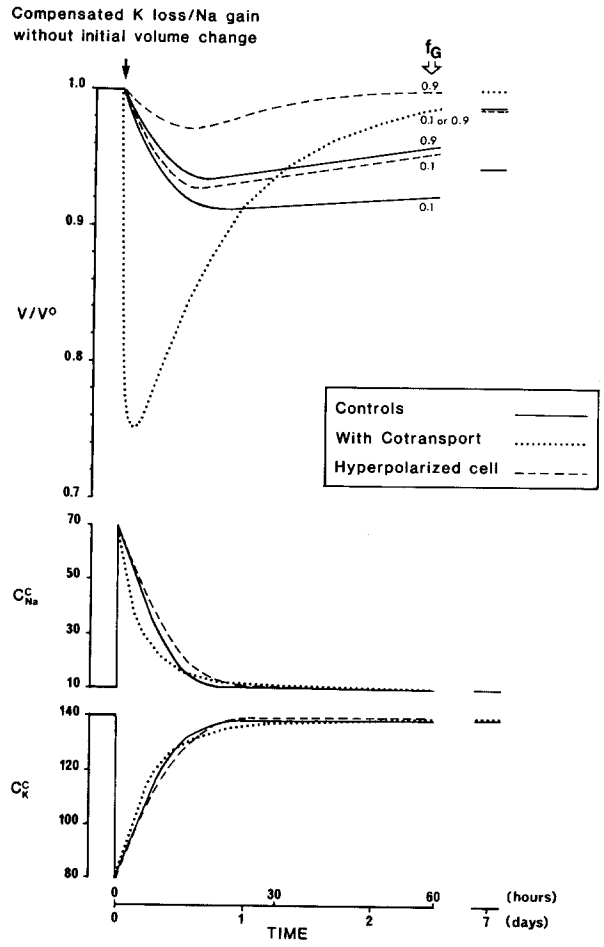

Fig. 3. Predicted time course of cell volume and Na/K concentration changes after a compensated dissipative change in cell Na/K concentrations. The insert lists the models considered and corresponding curves. f_G refers to kinetic variants with 10% (0.1) and 90% (0.9) electrodiffusive flux components for passive Na/K transport

courses for the recovery of the cell Na and K concentrations are roughly similar, and that by about 15 hours recovery is more than 95% complete. The pattern of the predicted volume changes, on the other hand, is substantially different for each of the models. In all cases cell dehydration occurs during concentration recovery, but its extent varies considerably. In control cells with 10% electrodiffusional Na and K flux-components, which probably represent best the condition of normal human red cells, the predicted volume reduction is small, being less than 9% of the original cell volume at its maximal extent. This occurs after about 15–20 hr of incubation and is consistent in timing and extent with the observations of Clark et al. [16]. Volume restoration, on the other hand, occurs over many weeks and was only 35% complete by the end of the first week. The extremely slow time course of volume restoration in red cells was first predicted by Tosteson [64] for sheep red cells in pioneering studies with a nonsteady-state transport red cell model. Figure 3 also shows that, in the absence of activated cotransport, (i) dehydration is slower and smaller in hyperpolarized cells than in control cells, (ii) in models with 90% electrodiffusional Na and K flux components cell dehydration is slower and smaller than in models with 10% electrodiffusion; this difference is more marked in hyperpolarized cells than in the controls, (iii) the smaller the extent of and time required for maximal dehydration, the faster the rate of volume restoration. All these effects were found to be negligibly affected by the value of the diffusional anion permeability within measured ranges. At the start of the incubation, the membrane potential was hyperpolarized by −1.5 to −2 mV relative to its value of −8.6 mV in the reference state with normal Na/K gradients. In the models with 10 and 90% electrodiffusional Na/K flux components maximal hyperpolarization was computed at 10 hr (−11.7 mV) and 25 hr (−10.8 mV), respectively. Hyperpolarization closely followed the time course of dehydration, and repolarization followed the time course of rehydration, not that of Na/K gradient recovery. If the simulations were performed with the Na pump fully inhibited and the Na : K : 2A cotransport inactive, there was neither hyperpolarization nor dehydration phase.

Since all isosmotic cell volume changes depend on the loss or gain of diffusible anion (*see* Appendix), the volume changes described above must depend on the driving forces governing net diffusive anion movements. We must therefore analyze these forces in detail. In the absence of cotransport-mediated fluxes, the Na-pump dependence of volume reduction shows that, as envisaged by Glader and Nathan [33] and observed by Clark et al. [16], the dehydration phase is linked to the activity of the electrogenic Na pump. Stimulation of the pump by the highly increased Na/K ratio caused the small but sharp initial hyperpolarization. The difference between the membrane potential and the Nernst potential of the diffusible anion represents the driving force for net anion flux. The initial pump-mediated hyperpolarization was small, but enough to secure that more than 98% of the excess Na efflux over K influx via the Na pump was balanced by net anion efflux through its electrodiffusional pathway. The resulting net Na + A efflux in excess of K + A gain accounts for cell dehydration. During this dehydration phase, the increasing concentrations of impermeant cell solutes, together with minor pH and nonideal osmotic effects (which will be analyzed in

detail with the third example), cause intracellular dilution of the diffusible anion as it exits the cell. This reduces the driving potential and hence the driving force for net anion efflux. Restoration of the Na/K gradients, on the other hand, tends to drive the membrane potential back to its reference state value. This initially contributes to reduction, and eventually causes reversal, of the driving force for net anion movement. Reversal of the driving potential in the direction of net anion gain sets up the volume restoration phase. The rate of rehydration is determined by the strength of this anion driving force, which is very small in red cells with normal membrane potential, but increases substantially in a hyperpolarized cell. Thus, the rate of volume restoration is determined by the magnitude of the electrodiffusional Na and K flux components and by the absolute value of the membrane potential. The overall size of the cation traffic across human and most other mammalian red cell membranes is so minute, and the membrane potential so small, that even if all the passive Na/K movements were electrodiffusional, the predicted time for complete volume restoration would exceed a week. In the more realistic instance of the electrodiffusive fluxes representing only a small fraction of the total passive fluxes, the time to full volume recovery would exceed the lifespan of many cells in any blood sample. The availability of techniques of long-term incubation of human red cells may now make it possible to test these alternatives [26]. In general, cells with high membrane potentials and with substantial electrodiffusive pathways for Na, K and Cl are better equipped to resist shrinkage and achieve earlier volume recovery following Na/K gradient dissipation than are tighter cells with lower potential. Human, and perhaps other mammalian red cells [64] would appear to be ill equipped for this type of volume regulation. The present analysis provides firm theoretical support for the conclusions of Clark et al. [16].

The membrane potential is not the only possible link between the fluxes of Na, K and A. Carrier-mediated cotransport of these ions has now been abundantly documented in a large variety of cells, including red cells [17, 22, 23, 36, 37, 50, 69]. The present analysis contributes the notion that even a relatively weak cotransport, which could speed up Na pump-mediated Na/K recovery only by a factor of two, for instance, could make a substantial contribution to the initial volume imbalance before contributing effectively to the volume restoration process. Na/K gradient dissipation will always drive a passive cotransporter, as defined here by Eq. (14), to net anion extrusion with consequent cell shrinkage. The rate, however, will depend on the precise kinetics of the cotransporter. A kinetics that would reduce such an effect without impairing the contribution to volume recovery would require the altered internal Na/K concentrations to inhibit the cotransporters' turnover. The recent discovery that this type of cotransport represents a major pathway in ferret red cells [23] may enable more direct studies of the kinetics of such a system.

The analysis thus far has demonstrated that delayed volume recovery following Na/K gradient dissipation is a basic property of human red cells, since it results from the low level of ionic traffic through pathways that link the fluxes of Na, K and Cl. Given these inbuilt constraints, delayed volume recovery is independent of the kinetics of transport through each of the individual transporters.

We consider next the possible relevance of this analysis to normal and abnormal red cells. The only normal condition claimed to cause ion-gradient dissipation is microcirculatory shear stress. Some apparent Ca-gradient dissipation has been described in vitro [51], but under conditions accompanied by some hemolytic damage. Because the Na/K gradients are so much smaller than those of Ca^{2+}, compensated dissipation of Na and K caused by shear stress may be too small to measure directly. If such episodes did occur in the capillary microcirculation, however, they should promote cell dehydration during gradient dissipation and while Na/K gradients are being restored. Volume restoration, on the other hand, would be too slow for meaningful rehydration between capillary passages. Therefore, as the red cells age, they may keep a cumulative record of those events in the form of a progressive, though probably very small, reduction in volume, without noticeable changes in Na and K concentrations. The normal age-related increase in red cell density might be based on this mechanism.

The best characterized abnormal condition causing substantial compensated Na/K dissipation is deoxygenation-induced sickling of *SS* red cells [66]. What the present results add to previous suggestions and observations [16, 33] is that cell dehydration may be expected to persist for weeks even if full recovery of the Na/K gradients had occurred within the first day. If the rate of sickling/desickling in the circulation exceeds a critical frequency, it is easy to see how gradient restoration between sickling events may be unable to oppose cumulative dissipation. Balanced Na/K gradient dissipation, however, fails to account for the fact that irreversibly sickled cells show a marked excess of K loss over Na gain [3], a state which cannot be attributed to Na-pump-mediated dehydration. This mechanism, therefore, does not appear to be a plausible working hypothesis to explain irreversible sickle cell forma-

tion, though it may contribute to cell dehydration, particularly in the initial stages.

Cell Volume and pH Changes Following Replacement of the Permeant Anion by an Impermeant Monovalent Anion

Formulation of the Problem

Phosphate buffers, isosmotic with plasma, or phosphate-buffered saline containing a substantial proportion of phosphate, were often used and are still recommended as suspending media for red cells in studies of hemoglobin function [*see*, for example, 21, 46, 49, 58, 62]. Bookchin et al. [4] recently showed that this treatment of the cells results in altered cell properties which were neither intended nor are appropriate for the attempted studies. The alterations consisted in transient cell alkalinization and rapid and sustained cell dehydration, which preceded any phosphate entry. Although the bases of the observed changes could be explained [4], it was not possible to predict the precise rate and extent of these effects under all the experimental conditions in which it was necessary or convenient to carry out such studies. The critical questions are: in the simplest case of a one-for-one replacement of the external diffusible anion by an impermeant monovalent anion, what determines the extent of cell dehydration and pH change to each level of impermeant anion in the medium? Can we use the measured changes in cell volume and pH in this type of experiments to determine some fundamental cell properties?

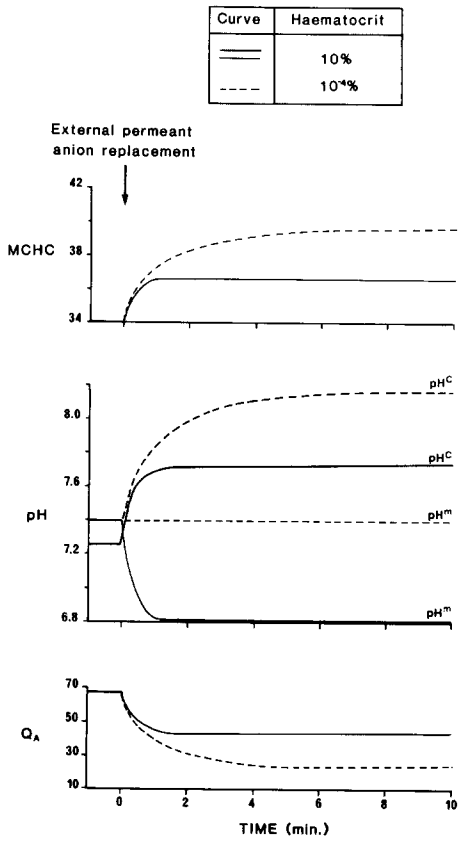

Fig. 4. Predicted effects of external anion replacement on cell volume and permeant anion content and on cell and medium pH, at two different hematocrits. At $t = 0$, all but 5 mM of the external permeant anion were replaced by a monovalent impermeant anion. For easier comparison with the results of Bookchin et al. [4], the mean corpuscular hemoglobin concentration (MCHC) rather than the relative volume (V/V_o) were used here to report cell volume. The relation between these two quantities is given in Eq. (D14)

Results and Analysis

In the simulated experiments of Fig. 4, all but about 5 mM of the external permeant anion, A, was stoichiometrically replaced by an impermeant anion, such as gluconate. We followed the changes in cell volume, pH and permeant anion content, and in external pH, at two different hematocrits, 10% and 10^{-4}%, equivalent to infinite dilution. In the last condition the medium becomes an invariant sink and the cells absorb all changes, which therefore become maximal. The reduction in external permeant anion concentration sets up an outward gradient of A which activates the ϕ_{HA} flux through the Jacobs-Stewart mechanism, as analyzed for Fig. 2 (*see* section on the "Structure of the Model"). This causes rapid net anion and proton loss from the cells, with opposite cell and medium pH changes. As anion is lost, the cells shrink. The predicted fluid loss is approximately isotonic in A, as observed [4]. The magnitude of these changes in the quasi steady-states that follow depends on the hematocrit, the composition and concentration of the external buffer and, when these are constant, exclusively on the protonization and nonideal osmotic behavior of the impermeant cell ion.

This last point is critical, because it provides an easy method to characterize these important properties of the impermeant cell ion in situ, in intact normal and abnormal red cells, in short-term experiments in which the metabolic state of the cells is not significantly changed. The method consists of measuring the hematocrit and pH of the cell suspension at different levels of permeant anion in the medium. The differences between measured and predicted quantities can then be used to search for the best-fit functional expressions and parameters in Eqs. (1) and (2). This method explores only the range of cell pH which is alkaline in relation to the pH in the medium before anion replacement.

With the next example we shall consider an alternative procedure to explore the acidic titration range. A preliminary comparison between the predicted results of Fig. 4 and those obtained by Bookchin et al. [4] (their Fig. 2) using citrate as an impermeant anion replacement shows excellent qualitative agreement, but also some minor quantitative discrepancies. Though the experimental conditions are not strictly comparable, it seems clear that for a similar fall in cell anion, the measured shrinkage and cell pH were higher than predicted from the description and parameters used here for Eqs. (1) and (2). This may mean that in these conditions the osmotic coefficient of hemoglobin is higher than previous estimates suggested, and that proton buffering by hemoglobin, at least in the alkaline range of cell pHs, is lower than what the nystatin equilibrium experiments suggested. It is not justified, however, to attempt to improve the fit or to pursue this analysis further without additional experiments. The brief analysis of the predictions in Fig. 4 illustrates the potential application and usefulness of the proposed method.

Effects of a Large and Sudden Increase in the Cell K Permeability in Low-K Media

Formulation of the Problem

A neutral K:H countertransport activated and modulated by the cytoplasmic Ca^{2+} concentration has been recently proposed by Cala [10, 11] to mediate a volume regulatory response of *Amphiuma* red cells. Although the evidence presented for the existence and operation of such a mechanism seems elegant and sound, several questions arise: are there any alternative interpretations of the data? What critical experimental tests could be designed to investigate the validity of any such alternatives? As we shall demonstrate, the answer to these questions relates to another group of very familiar experiments with red cells, in which the diffusional K permeability of the cell membrane can be rapidly and selectively increased by up to four orders of magnitude, either by incorporation of the K-selective ionophore valinomycin [42, 43] or by activation of endogenous Ca^{2+}-sensitive K channels present in red cells from many species [60]. When the K permeability is thus increased, with the cells suspended in low-K, Cl^--containing media, the cells hyperpolarize and, following the net loss of K and Cl^-, dehydrate at a rate limited by the diffusional anion permeability [40–43, 52]. These effects are familiar, well characterized, and easy to interpret. Possible alternative interpretations of Cala's experiments are related to the following questions: if the increased K permeability is purely electrodiffusional, does cell pH change? Are the K and Cl losses comparable? Is the fluid lost from the cells isotonic? How should anion carrier inhibitors affect net K and Cl losses? How does the membrane potential change in time? What are the effects, in each case, of replacing Cl ions by anions with less limiting diffusional permeabilities, such as SCN^- [56]? The answers to these questions are virtually impossible to predict in the absence of an intregrated model.

We could also adapt the questions of the previous example to the experiments considered here. When the anion permeability is not limiting, what determines the extent of dehydration of K-permeabilized red cells at different external K levels? What would the hematocrit and medium pH changes be in this case? What is the essential difference between these conditions and those of the impermeant anion replacement experiments?

Results and Analysis

The experiments in Fig. 5 were simulated at 10% hematocrit. They predict the changes in a number of variables over the first hour following a 10^3–10^4 increase in the K permeability of the cells in the presence of anions of increasing diffusional permeability, from 0.2 hr^{-1}, equivalent to that reported for Cl ions in human red cells [9, 35, 42, 43], to about 10^3 times this value. It can be seen that when the diffusional anion permeability is about a hundred times that reported for Cl^-, the anion permeability is no longer limiting to the rate of K loss. The diffusional anion permeability determines not only the rates of K and A loss, but also the pattern of change in membrane potential [28, 63]. With normal anion permeability, hyperpolarization is maximal at the onset of the K permeability increase, as a result of the increased Goldman potential determined by the new ratio of the increased diffusional permeability of K to that of A. In the presence of a nonlimiting anion, the initial hyperpolarization due to the Goldman potential is minimal; but the membrane potential increases rapidly as the cell dehydrates, because the Donnan potential rises with the concentration of impermeant anions in cell water. At normal or low anion permeabilities, the transition from Goldman to Donnan potentials as the cell dehydrates is slower and appears as a more or less steady hyperpolarization. However, this steadiness of the potential may be deceptive because at the same time substantial changes in cell volume, composition, and pH are taking place. The increase in Donnan potential with cell dehydration occurs de-

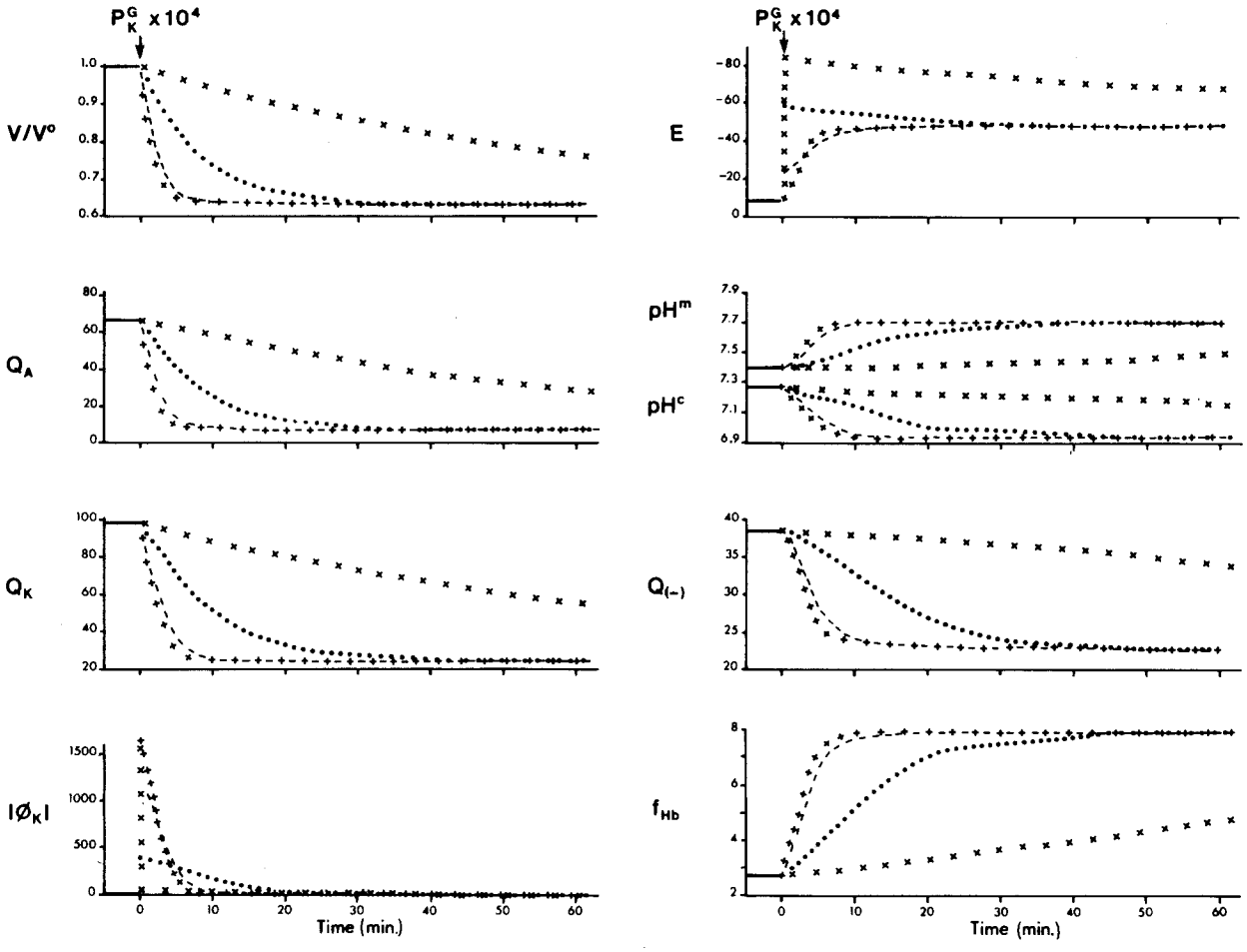

Curve	P_A^G (h^{-1})
×××××××	0.2
·····	2.0
-------	20
+++++++	200

Fig. 5. Predicted effects of a sudden increase in the diffusional K permeability in the presence of permeant anions of different diffusional permeability. All experiments were simulated at 10% hematocrit

spite a fall in total negative charge per liter original cells, $Q_{(-)}$, as explained below.

At nonlimiting anion permeabilities all changes appear complete within about 10–20 min. This is not, however, a true steady-state, for slower changes, involving Na-pump fluxes stimulated by the increased Na concentration within the shrunken cells, continue beyond the initial period of rapid changes. Since long term predictions are not under consideration here, the analysis will be confined to the rapid changes and quasi steady-states of the first 15–30 min in conditions where the anion permeability is not limiting.

Comparison of the Q_A and Q_K curves in Fig. 5 shows that more K than A is lost from the cells. The pH curves show that K loss is accompanied by cell acidification and medium alkalinization. Since the net Na flux is negligible and outwards, proton influx must provide the balancing charge for the excess K efflux over A efflux. If the loss of K and A had been isotonic, the expected loss of cell water would have been $\Delta V_w = (\Delta Q_K + \Delta Q_A)/\Sigma\, C_i^m = 0.53$ liter/loc in the quasi steady-state. The loss of cell water observed in the simulated experiments was only 0.35 liter/loc. This indicates that the fluid lost was hypertonic relative to medium tonicity. The model there-

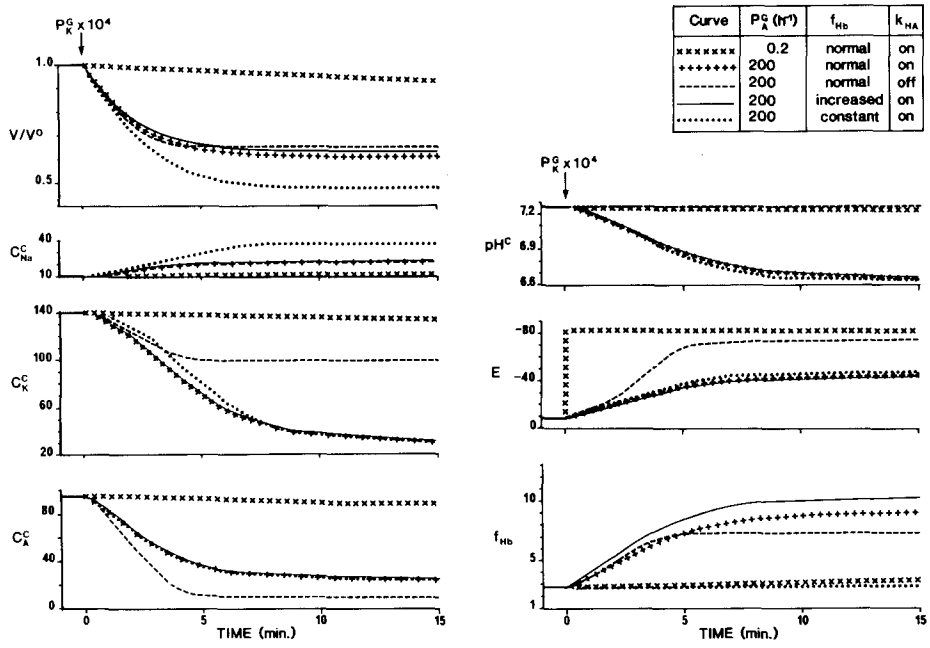

Fig. 6. Effects of the operation of the Jacobs-Stewart cycle and of changes in the osmotic coefficient of hemoglobin on the predicted behavior of model variables after a sudden increase in the diffusional K permeability. The value of the virial coefficient c in the curves with increased osmotic coefficient was raised from 0.026 to 0.04. All simulations were performed at 10^{-4}% hematocrit

fore predicts that activation of a K permeability in low-K media will cause cell acidification and the loss of an hypertonic fluid containing an excess of K over A.

The mechanism for these predicted effects becomes clear from the analysis of the curves in Fig. 6. These experiments were simulated at infinite cell dilution to focus attention on cell mechanisms only. The osmotic effects were analyzed by comparing curves with the osmotic coefficient of hemoglobin set at either normal, increased, or constant values. The normal and increased settings correspond, respectively, to the values of virial coefficients from Table 1 or to the highest estimates reported by McConaghey and Maizels [59] (*see* legend of Fig. 6). The "constant" setting represents ideal osmotic behavior in the sense that the osmotic coefficient of hemoglobin is independent of cell volume and remains at its reference state value (*see* Table 2) throughout the experiment. It can be seen that the predicted fluid loss becomes isotonic only when the coefficient is constant. This means that hypertonicity of the fluid leaving the cells can be ascribed entirely to the nonideal osmotic behavior of hemoglobin. Whereas the difference in cell dehydration between "constant" and nonideal conditions is large, that between middle and extreme range values for the virial coefficients is relatively small.

A comparison of the two curves with the Jacobs-Stewart mechanism "on" or "off" shows that cell acidification and the excess loss of K over A occur only when the mechanism is operational. Figure 6 also shows that under all conditions A loss is accompanied by dilution of A. These results suggest the following mechanisms for cell acidification and excess loss of K over A. K permeabilization causes the membrane potential to hyperpolarize, from its reference state value at the equilibrium potential of the diffusible anions to a value intermediate between the equilibrium potentials of K and of the diffusible anions. This creates the potential gradient which drives A out of the cell following the K loss down its concentration gradient. K and A comprise nearly all the osmotically active solvents in the cell effluent. To secure isotonicity between this effluent and the fluid within the cell the molar ratio of K and A to water in the effluent must be higher than it is in the cells where other solutes contribute to the internal osmolarity. Hence, loss of cell K and A must reduce not only their content per unit hemoglobin but also their concentration in cell water. Upon reduction in cell A concentration, an increase in r_A generates a driving force for H ion influx through the Jacobs-Stewart mechanism, leading to restoration of $r_H = r_A$, with cell acidification. The number of protons gained by the cells will depend entirely on the nature and concentration of the cell buffer. For an equivalent initial dilution of A, the more highly buffered the cells, the more protons will have to enter to restore the equality of H^+ and A concentration ratios. Titration of the cell buffer, in turn, will remove fixed negative charges and retain A within the cells, thus opposing further cell dehydration. If the proton shifts are blocked, as represented by the curve with k_{HA} off, the concentration of unbuffered fixed cell anions will increase more steeply

with cell dehydration, creating a larger Donnan potential, with higher K and lower A concentrations in the quasi-steady state. This leads to the interesting prediction that, if it were possible to block the anion carrier without severely reducing the diffusional permeability of a nonlimiting anion, then increasing the K permeability (with valinomycin, for instance) should cause more loss of A than in controls without anion carrier inhibitors.

In the quasi-steady states generated by K permeabilization, as with the anion replacement experiments, cell volume and pH are determined by the charge and nonideal osmotic properties of hemoglobin. Unlike with the anion replacement experiments, however, under conditions of K permeabilization the cells acidify. Therefore, the latter conditions can be used to investigate those properties of hemoglobin in the acidic pH range.

We can now attempt a possible reinterpretation of Cala's [10, 11, 12] results based on the previous analysis. As shown above, an excess K over A loss together with a charge-balancing influx of protons is expected whenever the K permeability is increased in low-K media. As demonstrated by the model, these effects neither require nor disprove the mediation of an electroneutral K : H exchanger. The predicted ratio of K to A loss in human red cells was within the range 1.3–2. In *Amphiuma* red cells the observed K loss in excess of Cl loss was about fivefold [11, 12]. To account for this excess in the absence of a K : H exchange mechanism, *Amphiuma* red cells would require 2–5 times the proton buffering capacity of normal human red cells. To our knowledge, measurement of this buffering capacity has not yet been reported. In view of these considerations, the strongest argument in support of an electroneutral K : H exchanger now rests on evidence for a low membrane conductance in conditions where the K flux was presumed to be activated [12]. Cala's findings, that the hyperpolarizing effect of valinomycin was similar with or without stimulation of the K fluxes, would appear to provide that evidence. Recent findings, however, demonstrate that the ionophore A23187 induces an extremely heterogeneous distribution of Ca in human red cells [56]. The results used by Cala ([11], *see* Figs. 2 and 3) to document Ca^{2+} dependence and modulation of the volume regulatory K flux, show a stepwise "all or none" pattern [57] which suggests that the Ca^{2+} distribution among the cells in which membrane potentials were measured with microelectrodes may also have been extremely heterogeneous. These considerations raise uncertainty about the assumption that the conductance and flux measurements were made on cells in strictly comparable states. The critical test would be to measure the above potentials and fluxes under conditions of confirmed uniformity and constancy of the intracellular Ca^{2+} distribution.

We wish to thank the Wellcome Trust Foundation and Medical Research Council of Great Britain and the National Institute of Health of the United States (grants HL28018 and HL21016) for funds. We are grateful to P.W. Flatman, A.M. Brown, H.G. Ferreira, J. Garcia-Sancho, A.S. Fruchter, J.D. Cavieres, and E. Hviid Larsen for helpful discussions and for reading the original drafts.

This paper is dedicated to the memory of Jens Otto Wieth, who performed, guided and inspired much of the work on which this analysis is based.

References

1. Adair, G.S. 1929. Thermodynamic analysis of the observed osmotic pressures of protein salts in solutions of finite concentration. *Proc. R. Soc. London A* **126:**16–24
2. Beauge, L., Lew, V.L. 1977. Passive fluxes of sodium and potassium across red cell membranes. *In:* Membrane Transport in Red Cells. J.C. Ellory and V.L. Lew, editors, pp. 39–51. Academic, New York
3. Bookchin, R.M., Lew, V.L. 1983. Red cell membrane abnormalities in sickle cell anemia. *In:* Progress in Hematology. Vol. 13. Elmer B. Brown, editor. Grune & Stratton, New York
4. Bookchin, R.M., Lew, D.J., Balazs, T., Ueda, Y., Lew, V.L. 1984. Dehydration and delayed proton equilibria of red blood cells suspended in isosmotic phosphate buffers. *J. Lab. Clin. Med.* **104:**855–866
5. Brewer, G.J., Oelshlegel, F.J., Jr., Schoomaker, E.B., Knutsen, C.A. 1972. Potential effects of hemoglobin concentration on red cell metabolism together with observations on red cell metabolic differences between men and women. *In:* Hemoglobin and Red Cell Structure and Function. C.J. Brewer, editor. pp. 99–119. Plenum, New York/London
6. Brugnara, C., Kopin, A.S., Brunn, H.F., Tosteson, D.C. 1984. Electrolyte composition and equilibrium in hemoglobin CC red blood cells. *Trans. Assoc. Am. Physicians* **97:**104–112
7. Brugnara, C., Kopin, A.S., Bunn, H.F., Tosteson, D.C. 1985. Regulation of cation content and cell volume in hemoglobin erythrocytes from patients with homozygous hemoglobin C disease. *J. Clin. Invest.* **75:**1608–1617
8. Brumen, M., Glaser, R., Svetina, S. 1979. Osmotic states of the red blood cell. *Bioelectrochem. Bioenerg.* **6:**227–241
9. Cabantchik, Z.I., Knauf, P.A., Rothstein, A. 1978. The anion transport system of the red blood cell. *Biochim. Biophys. Acta* **515:**239–302
10. Cala, P.M. 1980. Volume regulation by *Amphiuma* red blood cells: The membrane potential and its implications regarding the nature of the ion-flux pathways. *J. Gen. Physiol.* **76:**683–708
11. Cala, P.M. 1983. Volume regulation by red blood cells: Mechanisms of ion transport. *Mol. Physiol.* **4:**33–52
12. Cala, P.M. 1983. Cell volume regulation by *Amphiuma* red blood cells. *J. Gen. Physiol.* **82:**761–784
13. Canessa, M., Brugnara, C., Cusi, D., Tosteson, D.C. 1986. Modes of operation and variable stoichiometry of the furosemide-sensitive Na and K fluxes in human red cells. *J. Gen. Physiol.* **87:**113–142

14. Cass, A., Dalmark, M. 1973. Equilibrium dialysis of ions in nystatin-treated cells. *Nature New Biol.* **244:**47–49
15. Cavieres, J.D. 1977. The sodium pump in human red cells. *In:* Membrane transport in red cells. J.C. Ellory and V.L. Lew, editors. pp.1–37. Academic, New York
16. Clark, M.R., Guatelli, J.C., White, A.T., Shohet, S.B. 1981. Study on the dehydrating effect of the red cell Na^+/K^+-pump in nystatin-treated cells with varying Na^+ and water contents. *Biochim. Biophys. Acta* **646:**422–432
17. Dagher, G., Brugnara, C., Canessa, M. 1985. Effect of metabolic depletion on the furosemide-sensitive Na and K fluxes in human red cells. *J. Membrane Biol.* **86:**145–155
18. Dalmark, M. 1975. Chloride and water distribution in human red cells. *J. Physiol. (London)* **250:**65–84
19. Dick, D.A.T. 1959. Osmotic properties of living cells. *Int. Rev. Cytol.* **8:**387–448
20. Dick, D.A.T., Lowenstein, L.M. 1958. Osmotic equilibria in human erythrocytes studied by immersion refractometry. *Proc. R. Soc. London B* **148:**241–256
21. Elbaum, D., Nagel, R.L., Bookchin, R.M., Herskovitz, T.T. 1974. Effect of alkylinease on the polymerization of hemoglobin S. *Proc. Natl. Acad. Sci. USA* **71:**4718
22. Ellory, J.C., Dunham, P.B., Logue, P.J. 1982. Anion-dependent cation transport in erythrocytes. *Phil. Trans. R. Soc. London B* **299:**483–495
23. Flatman, P.W. 1983. Sodium and potassium transport in ferret red cells. *J. Physiol. (London)* **341:**545–557
24. Flatman, P.W., Lew, V.L. 1980. Magnesium buffering in intact human red blood cells measured using the ionophore A23187. *J. Physiol. (London)* **305:**13–30
25. Fortes, P.A.G. 1977. Anion movements in red blood cells. *In:* Membrane Transport in Red Cells. J.C. Ellory and V.L. Lew, editors. pp. 175–195. Academic, New York
26. Freedman, J.C. 1983. Partial requirements for *in vitro* survival of human red blood cells. *J. Membrane Biol.* **75:**225–231
27. Freedman, J.C., Hoffman, J.F. 1979. Ionic and osmotic equilibria of human red blood cells treated with nystatin. *J. Gen. Physiol.* **74:**157–185
28. Freedman, J.C., Hoffman, J.F. 1979. The relation between dicarbocyanine dye fluorescence and the membrane potential of human red blood cells set at varying Donnan equilibria. *J. Gen. Physiol.* **74:**187–212
29. Frumento, A.S. 1965. The electrical effects of an ionic pump. *J. Theor. Biol.* **9:**253–262
30. Funder, J., Wieth, J.O. 1966. Chloride and hydrogen ion distribution between human red cells and plasma. *Acta Physiol. Scand.* **68:**234–235
31. Gary-Bobo, C.M., Solomon, A.K. 1968. Properties of hemoglobin solutions in red cells. *J. Gen. Physiol.* **52:**825–853
32. Gary-Bobo, C.M., Solomon, A.K. 1971. Hemoglobin charge dependence on hemoglobin concentration *in vitro*. *J. Gen. Physiol.* **57:**283–289
33. Glader, B.E., Nathan, D.G. 1978. Cation permeability alterations during sickling: Relation to cation composition and cellular hydration of irreversibly sickled cells. *Blood* **51:**983–989
34. Glynn, I.M. 1985. The Na^+,K^+-transporting adenosine triphosphatase. *In:* The Enzymes of Biological Membranes. A.N. Martonosi, editor. pp. 35–114. Plenum, New York/London
35. Glynn, I.M., Warner, A.E. 1972. Nature of the calcium dependent potassium leak induced by (+)-propranolol, and its possible relevance to the drug's antioarrhythmic effect. *Br. J. Pharmacol.* **44:**271
36. Haas, M., Schmidt, W.F., III., McManus, T.J. 1982. Catecholamine-stimulated ion transport in duck red cells. *J. Gen. Physiol.* **80:**125–147
37. Hall, A.C., Ellory, J.C. 1985. Measurements and stoichiometry of bumetanide-sensitive (2Na : 1K : 3Cl) cotransport in ferret red cells. *J. Membrane Biol.* **85:**205–213
38. Hladky, S.B., Rink, T.J. 1977. pH equilibration across the red blood cell membrane. *In:* Membrane Transport in Red Cells. J.C. Ellory and V.L. Lew, editors. pp. 115–135. Academic, London
39. Hladky, S.B., Rink, T.J. 1978. Osmotic behaviour of human red blood cells: An interpretation in terms of negative intracellular fluid pressure. *J. Physiol. (London)* **274:**437–446
40. Hoffman, J.F., Laris, P.C. 1974. Determinations of membrane potentials in human and *Amphiuma* red blood cells by means of a fluorescent probe. *J. Physiol. (London)* **239:**519–552
41. Hoffman, J.F., Lassen, U.V. 1971. Plasma membrane potentials in amphibian red cells. *Proc. Int. Union Physiol. Sci.* **9:**253 (*Abstr.*)
42. Hunter, M.J. 1971. A quantitative estimate of the non-exchange restricted chloride permeability of the human red cell. *J. Physiol.* **218:**49*P*
43. Hunter, M.J. 1977. Human erythrocyte anion permeabilities measured under conditions of net charge transfer. *J. Physiol. (London)* **268:**35–49
44. Hviid-Larsen, E. 1978. Computed steady-state ion concentrations and volume of epithelial cells. Dependence on transcellular Na^+ transport. Alfred Benzon Symposium, Vol. 11, pp. 438–456. Copenhagen, Munksgaard
45. Hviid-Larsen, E., Kristensen, P. 1978. Properties of a conductive cellular chloride pathway in the skin of the toad (*Bufo bufo*). *Acta Physiol. Scand.* **102:**1–21
46. Imai, K. 1981. Measurement of accurate oxygen equilibrium curves by an automatic oxygenation apparatus. *Methods Enzymol.* **76:**438
47. Jacobs, M.H., Stewart, D.R. 1942. The role carbonic anhydrase in certain ionic exchanges involving the erythrocyte. *J. Gen. Physiol.* **25:**539–552
48. Jacobs, M.H., Stewart, D.R. 1947. Osmotic properties of the erythrocyte. XII. Ionic and osmotic equilibria with a complex external solution. *J. Cell. Comp. Physiol.* **30:**79–103
49. Kon, K., Maeda, N., Sekiya, M., Shiga, T., Suda, T. 1980. A method for studying oxygen diffusion barrier in erythrocytes: Effects of haemoglobin content and membrane cholesterol. *J. Physiol. (London)* **309:**569
50. Kregenow, F.M. 1977. Transport in avian red cells. *In:* Membrane Transport in Red Cells. J.C. Ellory and V.L. Lew, editors. pp. 383–426. Academic, New York
51. Larsen, F.L., Katz, S., Roufogalis, B.D., Brooks, D.E. 1981. Physiological shear stresses enhance the Ca^{2+} permeability of human erythrocytes. *Nature (London)* **294:**667–668
52. Lassen, U.V. 1972. Membrane potential and membrane resistance of red cells. *In:* Oxygen affinity of hemoglobin and red cell acid base status. M. Rørth and P. Astrup, editors. pp. 291–304. Academic, New York
53. Lauf, P.K. 1985. $K^+ : Cl^-$ cotransport: Sulfhydryls, divalent cations, and the mechanism of volume activation in a red cell. *J. Membrane Biol.* **88:**1–13
54. Lew, V.L., Beauge, L. 1979. Passive cation fluxes in red cell membranes. *In:* Membrane Transport in Biology. G.

Giebisch, D.C. Tosteson, and H.H. Ussing, editors. Springer-Verlag, Berlin
55. Lew, V.L., Ferreira, H.G., Moura, T. 1979. The behaviour of transporting epithelial cells. I. Computer analysis of a basic model. *Proc. R. Soc. London B* **206:**53–83
56. Lew, V.L., Garcia-Sancho, J. 1985. Use of the ionophore A23187 to measure and control cytoplasmic Ca^{2+} levels in intact red cells. *Cell Calcium* **6:**15–23
57. Lew, V.L., Maullem, S., Seymour, C.A. 1982. Properties of the Ca^{2+}-activated K^+ channel in one-step inside-out vesicles from human red cell membranes. *Nature (London)* **296:**742–744
58. Lian, C.Y., Roth, S., Harkness, D.R. 1971. The effect of alteration of intracellular 2,3-DPG concentration upon oxygen binding of intact erythrocytes containing normal and mutant hemoglobins. *Biochem. Biophys. Res. Commun.* **45:**151
59. McConaghey, P.D., Maizels, M. 1961. The osmotic coefficients of haemoglobin in red cells under varying conditions. *J. Physiol. (London)* **155:**28–45
60. Sarkadi, B., Gardos, G. 1985. Calcium-induced potassium transport in cell membranes. *In:* The Enzymes of Biological Membranes. A.N. Martonosi, editor. pp. 193–234. Plenum, New York/London
61. Savitz, D., Sidel, V.W., Solomon, A.K. 1964. Osmotic properties of human red cells. *J. Gen. Physiol.* **48:**79–94
62. Seakins, M., Gibbs, W.N., Milner, P.F., Bertles, J.F. 1973. Erythrocyte Hb-S concentration. An important factor in the low oxygen affinity of blood in sickle cell anemia. *J. Clin. Invest.* **52:**422
63. Simons, T.J.B. 1976. Carbo cyanine dyes inhibit Ca-dependent K efflux from human red cell ghosts. *Nature (London)* **264:**467–469
64. Tosteson, D.C. 1964. Regulation of cell volume by sodium and potassium transport. *In:* The cellular functions of membrane transport. J.F. Hoffman, editor. pp. 3–22. Prentice Hall
65. Tosteson, D.C., Hoffman, J.F. 1960. Regulation of cell volume by active cation transport in high and low potassium sheep red cells. *J. Gen. Physiol.* **44:**169–194
66. Tosteson, D.C., Shea, E., Darling, R.C. 1952. Potassium and sodium of red blood cells in sickle cell anemia. *J. Clin. Invest.* **31:**406–411
67. Whittam, R. 1964. *In:* Transport and Diffusion in Red Blood Cells. pp. 76–96. Edward Arnold, London
68. Wieth, J.O. 1970. Effects of monovalent cations on sodium permeability of human red cells. *Acta Physiol. Scand.* **79:**76–87
69. Wiley, S.J., Cooper, R.A. 1974. A furosemide-sensitive cotransport of sodium plus potassium in the human red cell. *J. Clin. Invest.* **53:**745–755

Received 2 January 1986; revised 25 March 1986

Appendix

Analysis of the Factors that Determine the Rate of Cell Volume Change (DV_w/Dt)

From the isotonicity condition (Eq. (17)), we obtain

$$Q_{NA} + Q_K + Q_A = V_w \Sigma C_i^m - (Q_{Mg} + f_{Hb}Q_{Hb} + Q_X). \quad \text{(A1)}$$

From the electroneutrality condition (Eq. (18)), we obtain

$$Q_{Na} + Q_K - Q_A = -(n_{Hb}Q_{Hb} + n_X Q_X + 2Q_{Mg}). \quad \text{(A2)}$$

Substracting Eq. (A2) from (A1) and rearranging, we obtain

$$2Q_A = V_w \Sigma C_i^m + (n_{Hb} - f_{Hb})Q_{Hb} + (n_X - 1)Q_X + Q_{Mg}. \quad \text{(A3)}$$

Differentiating both sides of Eq. (A3) in relation to time, substituting Eq. (1) and definition (2), and applying the conversion $Df_{Hb}/Dt = (Df_{Hb}/DV_w)(DV_w/Dt)$, we obtain

$$DV_w/Dt = (2\phi_A - aQ_{Hb}(DpH^c/Dt))/(\Sigma C_i^m - Q_{Hb}(Df_{Hb}/DV_w)) \quad \text{(A4)}$$

for conditions in which Q_{Mg}, n_X, Q_{Hb}, Q_X, pI and ΣC_i^m are constant in time.

Equation (A4) states that, at constant tonicity in the medium, the rate of change in red cell volume is determined by the factors which control the diffusible anion flux and cell pH and is modulated by the cell volume dependence of the osmotic coefficient of hemoglobin. Since Df_{Hb}/DV_w is negative, the effect of the nonideal osmotic behavior of hemoglobin is to reduce the rate of volume change more the smaller the cell volume.